Astrophysical Masers and their Environments
Proceedings IAU Symposium No. 242, 2007
J.M. Chapman & W.A. Baan, eds.

doi:10.1017/S1743921307013166

OH (1720 MHz) masers: signposts of SNR/molecular cloud interactions

Crystal L. Brogan

National Radio Astronomy Observatory, 520 Edgemont Rd, Charlottesville, VA, 22903, USA
email:cbrogan@nrao.edu

Abstract. Over the last decade it has been demonstrated that supernova remnant (SNR) OH (1720 MHz) masers are unique tracers of SNR/molecular cloud interactions. Here I briefly review the current state of our observational understanding of these masers including results from recent MERLIN and VLBA full polarization studies of the masers in W28, W44, and W51C. Some of our findings include that (1) in accordance with theory, the linear polarization position angles are either parallel or perpendicular to the plane-of-sky magnetic field determined through other observations; (2) the maser spot sizes are fairly large ($\sim 10^{14}$ cm) and exhibit a core/halo morphology; and (3) while the magnetic field strengths do increase slightly with higher resolution, this effect can be completely explained by spectral/spatial blending.

Keywords. Masers,(ISM:) supernova remnants

1. Introduction

Although "anomalous" OH (1720 MHz) emission toward a supernova remnant (SNR) was first identified in 1968 (Goss & Robinson 1968), this phenomenon was essentially ignored until Frail, Goss, & Slysh (1993) conclusively identified the emission toward W28 as arising from a maser process, and suggested that these masers may trace sites of SNR/molecular cloud interactions. This suggestion was supported by the earlier work of Elitzur(1976) that showed that OH (1720 MHz) masers can be collisionally pumped under the conditions present in such interactions. A number of surveys have subsequently been carried out toward most of the known SNRs in the Galaxy, as well as toward the Galactic Center region by Frail *et al.* (1996), Green *et al.* (1997), Yusef-Zadeh *et al.* (1996), Yusef-Zadeh *et al.* (1999), Koralesky *et al.* (1998). From these surveys OH (1720 MHz) masers have been found in $\sim$ 20 SNRs, or 10% of the known SNRs in our Galaxy. Interestingly, all of the OH (1720 MHz) SNRs are located towards the inner Galaxy ($l = \pm 50°$) where most of the molecular gas resides except one (IC443). SNR OH (1720 MHz) masers exhibit a number of characteristics that are distinct from OH (1720 MHz) masers observed in H II regions. For example, the SNR variety spot sizes tend to be several orders of magnitude larger (Claussen *et al.* 2002, Hoffner *et al.* 2003), have narrow simple line profiles, and have significantly weaker linear and circular polarization percentages of $\sim$ 10%. SNR OH (1720 MHz) masers have not been observed to be accompanied by any other maser species (see for example Claussen *et al.* 1999b).

More detailed analysis of the pumping mechanism for SNR OH (1720 MHz) masers suggest that they form in the post-shock molecular gas behind C-type shocks, and that a sufficient column of OH with the necessary velocity coherence can only be achieved if the shock is moving (more or less) transverse to the line of sight (Lockett *et al.* 1999; Wardle 1999). The X-rays from the SNR are a critical ingredient in these theories, as they induce the conversion of the most abundant species formed in post C-shock gas H_2O, to OH with about a 1% efficiency. These theories suggest that the collisional pump is only efficient

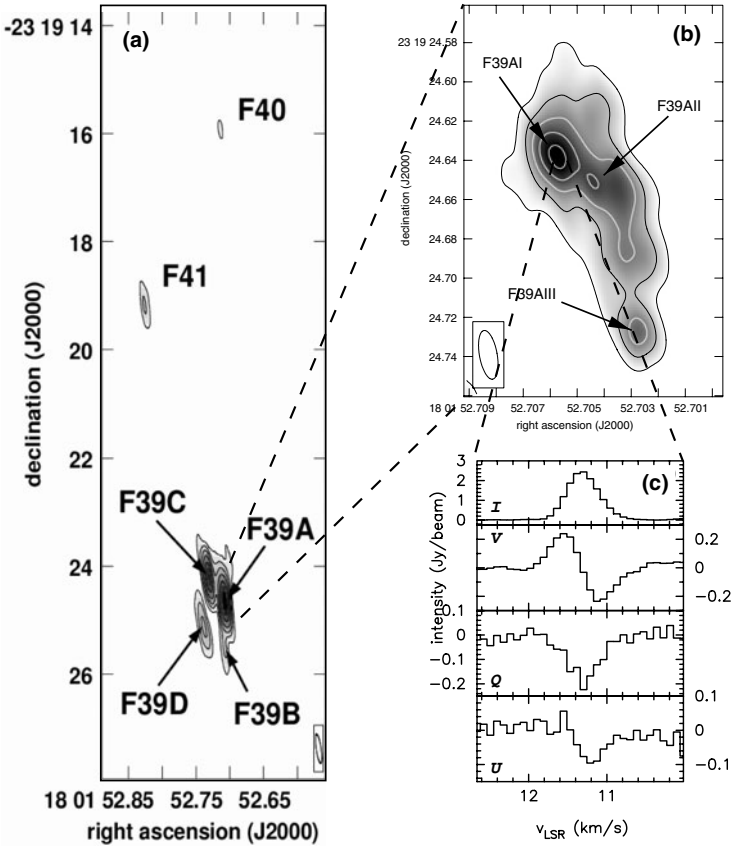

Figure 1. (a) MERLIN image of the W28 maser regions F39-41 with 550×100mas resolution (P.A. °). (b) VLBA image of the F39A masers with 25×9 mas resolution (P.A. 10°). (c) VLBA full polarization spectra of region F39AI. These figures are from Hoffman *et al.* (2005a).

over a very limited range of densities $\sim 1 \times 10^{(4-5)}$ cm^{-3} and temperatures in the range 50 K $< T <$ 125 K. Hence, observations of this OH maser line can indeed serve as a diagnostic probe of SNR/molecular cloud interactions. Moreover, since OH has a strong Zeeman coefficient at 1720 MHz (0.65 Hz μG^{-1}) it can also provide a powerful probe of the magnetic field strength in the post-shock molecular gas. Assuming the standard thermal Zeeman equation is appropriate for these masers, magnetic field strengths in the 0.2 – 5 mG range have been observed using the Very Large Array (VLA) (Claussen *et al.* 1997, Koralesky *et al.* 1998, Yusef-Zadeh *et al.* 1999, Brogan *et al.* 2000).

Although circa 2000, much had been learned about the distribution and general physical conditions accompanying OH (1720 MHz) masers using instruments like the Very Large Array (VLA) and Australia Telescope Compact Array (ATCA), a deeper understanding would require full polarization data obtained at high spatial resolution. Some of the key remaining questions include: (1) What are the detailed properties of the polarization, and what do they tell us about the strength and orientation of the 3-D magnetic field? (2) How is the maser flux distributed on small size scales and what are the true brightness temperatures? (3) Does the magnetic field strength increase when observed with higher resolution as might be expected if the magnetic fields are tangled on larger sizescales?

https://doi.org/10.1017/S1743921307013166 Published online by Cambridge University Press

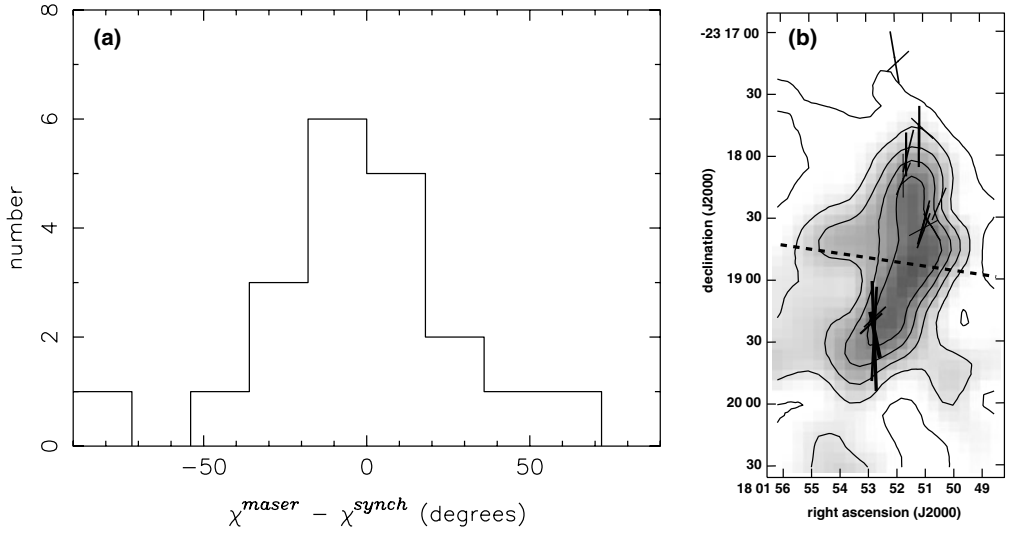

Figure 2. (a) Difference between χ^{synch} and χ^{maser} position angles. (b) Comparison between molecular shock morphology traced by CO(3–2) (in greyscale and contours) and the magnetic field direction defined by χ^{maser} rotated by 90° as suggested by similarity in $\chi^{synch} = 80°$ (dashed line) and χ^{maser}. These figures are from Hoffman *et al.* (2005a).

2. MERLIN and VLBA studies of OH (1720 MHz) maser sources

2.1. *SNR: W28*

The W28 SNR is located at a distance of $\sim$ 2.5 kpc (Velazquez *et al.* 2002) and is partially encircled by shocked molecular gas on its northern and eastern sides. Several regions of OH (1720 MHz) maser emission are coincident with the shocked molecular gas, with the strongest masers located toward the NE in regions denoted E and F (Claussen *et al.* 1997). Figure 1a shows the morphology of the W28 masers located in region F39-F41 observed with MERLIN, and Figure 1b shows the morphology of the F39A maser observed with the VLBA from the recent study by Hoffman *et al.* 2005a. Comparison between the total maser flux densities recovered from the VLA (Claussen *et al.* 1997) vs. MERLIN (Hoffman *et al.* 2005a) data yield a range of results. For example, essentially all of the VLA maser flux density from regions E31 and F39 is recovered in the MERLIN images. In contrast, many of the other maser spots have MERLIN flux densities that are 50%–75% less than measured with the VLA. These results suggest that at least some of the masers have structure on scales $> 3''$ (7,500 AU). A similar comparison between the MERLIN and VLBA flux densities reveal that the VLBA recovers 20%−85% of the MERLIN flux density. Overall these results suggest a core/halo morphology for SNR OH (1720 MHz) masers, but with a wide range of cutoff scalesizes (also see Yusef-Zadeh *et al.* 2003, and J. Hewitt *et al.* these proceedings).

VLBA spectral line profiles for all four Stokes parameters for the F39AI maser are shown in Figure 1c. The percent linear polarization for the MERLIN data ranges from 2%−22%, with an average value of 6% (over 20 distinct measurements). The measured Zeeman magnetic field strength B_θ ranges from 0.2 to 1.2 mG, assuming the thermal Zeeman equation (with no θ dependence). Comparison between the MERLIN data and the few spots with sufficient sensitivity for analysis show no trends in B_θ with increased resolution, beyond that expected from spatial blending of spots with slightly different v_{lsr}. For example, the VLBA line center velocities observed for the F39AI, II, III maser spots

https://doi.org/10.1017/S1743921307013166 Published online by Cambridge University Press

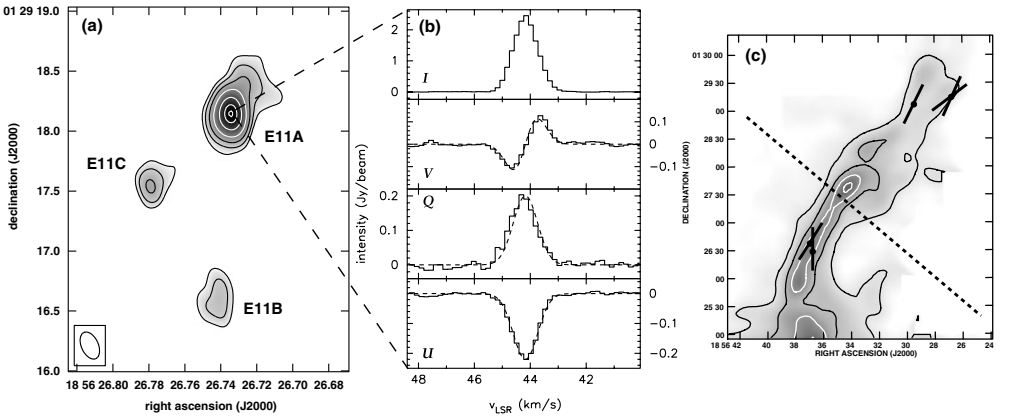

Figure 3. (a) MERLIN image. (b) MERLIN full polarization spectra. (c) Comparison between molecular shock morphology traced by CO(3–2) (in greyscale and contours) and the magnetic field direction defined by χ^{maser} (solid black lines). The dotted black line shows the position angle of $\chi^{synch} = 55°$. These figures are from Hoffman *et al.* (2005b)

differ by only 0.1 km s^{-1}, a factor of 14 times smaller than the range observed across the F39A,B,C,D masers at MERLIN scales. The low velocity dispersion observed at VLBA scales is an indication that this resolution ($\sim$ 25 AU, 4×10^{14} cm) is approaching the intrinsic scalesize of OH (1720 MHz) maser spots.

The position angle of the synchrotron linear polarization χ^{synch} has been measured on 2′ scales by Dickel & Milne(1976) to be $\sim 80°$. The Faraday rotation in the vicinity of the masers is estimated by these authors to be less than $\sim 20°$, it is also notable that χ^{synch} is quite uniform throughout the eastern and NE parts of the SNR. Figure 2a shows the difference between χ^{synch} and the maser linear polarization position angles χ^{maser}. This distribution is strongly peaked at a difference of 0°. Since synchrotron linear polarization is perpendicular to the plane of sky direction of the magnetic field ($B_\perp$), this comparison suggests that the maser linear polarization for this source is also perpendicular (with the caveat that the scalesizes of the observations are quite different). A comparison between the morphology of the shocked molecular filament in which the masers are immersed (Frail & Mitchell 1998) and the χ^{maser} *rotated by* 90° is shown in Figure 2b (a line indicating the *unrotated* χ^{synch} is also shown). The evident agreement with the rotated χ^{maser} suggests that for W28 $B_\perp$ is aligned with the long axis of the filament in agreement with expectation since only the component of the field parallel to the shock front will be compressed and amplified.

2.2. *SNR: W44*

The W44 SNR is located at a distance of 3.2 kpc (see for example Wolszczan *et al.* 1991) similar to W28 and has its strongest OH (1720 MHz) maser emission on its northeastern side. Figure 3a shows a MERLIN image of the W44 E11 region (maser spot E11A is also detected with the VLBA, but is unresolved). These data are from the recent MERLIN and VLBA study by Hoffman *et al.* (2005b). Similar to W28, the flux density measured for one maser group (C8) in the MERLIN data includes all of the VLA flux density observed by Claussen *et al.* (1997), but the MERLIN data are missing more than half the VLA flux density for most of the other maser spots. The VLBA data contain 50%−70% of the MERLIN flux density. This result provides another indication that SNR OH (1720 MHz) masers have a core/halo morphology.

Figure 3b shows MERLIN spectra of all four Stokes polarization parameters for the

https://doi.org/10.1017/S1743921307013166 Published online by Cambridge University Press

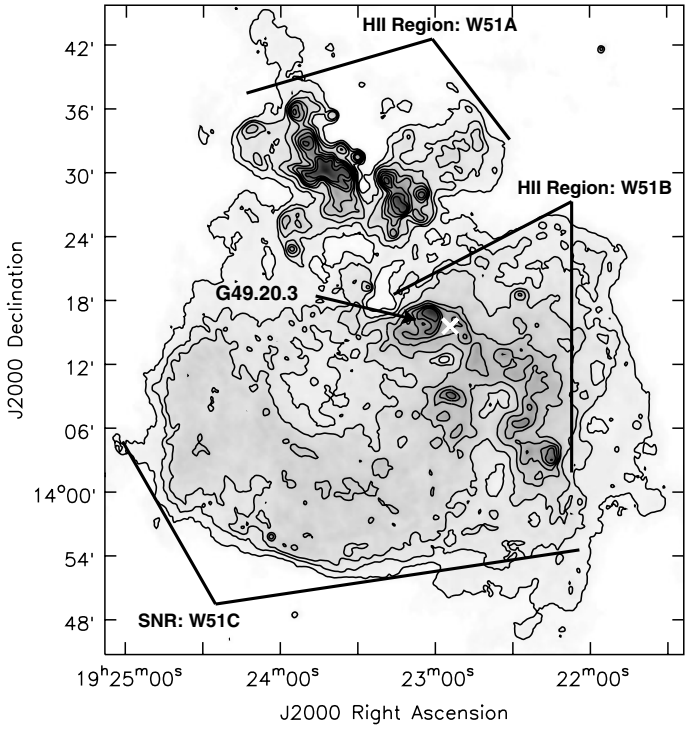

Figure 4. VLA 90cm image (greyscale and contours) of the W51 complex with 34″ resolution. The contour levels are 20, 60, 90, 150, 210, 300, 400, and 500 mJy beam^{-1}. The sources corresponding to W51 A, B, and C; as well as the ultracompact H II region G49.2-0.3 are labeled. The position of the OH (1720 MHz) masers is indicated by a white x symbol (Brogan et al. in prep.).

E11A maser. The magnetic field strengths measured from the MERLIN data are similar to the VLA measurements by Claussen *et al.* (1997), after accounting for a factor of two error in the Zeeman equation used by these authors. Unfortunately, the low signal-to-noise of the VLBA detections preclude measurement of the Zeeman magnetic field strengths. The percentage of linear polarization in the MERLIN data range from $7\% - 14\%$, similar to W28. Figure 3c shows the orientations of χ^{maser} compared to the linear filament of shocked CO(3–2) emission observed by Frail & Mitchell (1998). Both the filament and χ^{maser} are approximately perpendicular to the orientation of $\chi^{synch} \sim 55^\circ$ as observed by Dickel & Milne 1976 with 2′ resolution. Like the case of W28, Dickel & Milne(1976) do not find evidence for significant Faraday rotation in the vicinity of the masers. Thus, the direction of the plane-of-sky magnetic field implied by the χ^{synch} is still parallel to the long axis of the filament. However, instead of χ^{maser} and χ^{synch} being along a similar position angle as with W28, in W44 the two position angles are perpendicular to each other, suggesting that χ^{maser} is parallel to $B_\perp$ in this case.

2.3. *W51B/C region*

W51 is composed of two large H II region complexes (W51A, and W51B), as well as the SNR W51C (see Figure 4). W51 is located near the Sagittarius arm tangent point at $\sim l = 49^\circ$ and $\sim b = 0.3^\circ$ and thus precise distances for these sources have been difficult to determine due to the severe velocity crowding in this direction, though the range is likely between 4-7 kpc. Soft X-ray absorption toward the W51B region compared to the

https://doi.org/10.1017/S1743921307013166 Published online by Cambridge University Press

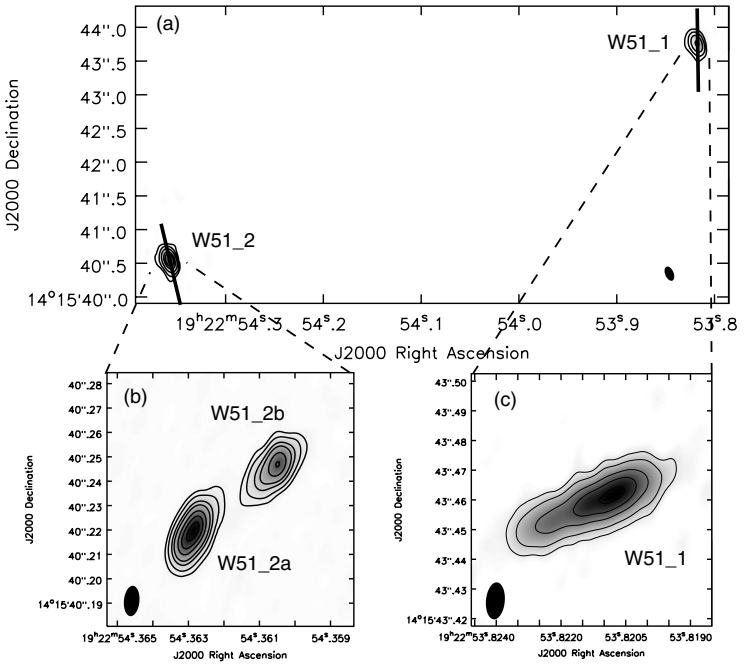

Figure 5. (a) MERLIN integrated intensity image (greyscale and contours) of maser spots W51C_1 and W51C_2. The contour levels are 70 (3σ), 200, 500, 1100, & 1700 mJy beam^{-1} km s^{-1}. The beam with a size of 225 × 126 mas P.A.= 23.0° is shown in the lower right. The straight solid lines indicate the linear polarization position angles. (b) VLBA integrated intensity image (greyscale and contours) of maser spots W51C_2a and W51C_2b. The contour levels are 50 (3σ), 100, 200, 300, 500, 700, & 900 mJy beam^{-1} km s^{-1}. (c) VLBA integrated intensity image (greyscale and contours) of maser spots W51C_1. The contour levels are 25 (3σ), 50, 100, 150, & 200 mJy beam^{-1} km s^{-1}. The beam with a size of 12.5 × 6.3 mas P.A.= −5.2° is shown in the lower left (Brogan et al. in prep.).

rest of the W51C SNR suggests that W51C lies behind W51B (Koo, Kim, & Seward 1995). The OH (1720 MHz) masers reported by Green et al. (1997) are located ∼ 2′ west of the W51B UCH II region G49.2-0.3. Despite this proximity, VLA observations of the W51 OH (1720 MHz) masers by Brogan et al. (2000) demonstrated that these masers share all the hallmarks of SNR OH (1720 MHz) masers, and like Green et al., conclude that they are most likely excited by the W51C SNR (the only known SNR in the region) and that the requisite molecular gas may be associated with the W51B H II region. The SNR OH (1720 MHz) masers in this region are denoted W51C_1 and W51C_2 to clearly distinguish them from the H II region OH (1720 MHz) masers in W51A (though it is not certain they are associated with W51C).

MERLIN and VLBA images of the W51C OH (1720 MHz) masers from Brogan et al. (2007, in preparation) are shown in Figure 5a,b,c. The B_θ magnetic field strengths measured for W51C_1 using MERLIN and the VLBA are both ∼ 1.5 mG, and coincidentally, this maser does not show significant substructure on VLBA scales. In contrast the MERLIN B_θ for W51C_2 (1.9 ± 0.1 mG) is intermediate between the values measured for the two VLBA maser spots, W51C_2a and W51C_2b: 1.7 ± 0.1 and 2.2 ± 0.1, respectively, that comprise W51C_2. As was true for W28, this difference is entirely consistent with the combined spectral/spatial blending present at the MERLIN resolution. The χ^{maser} measured from the MERLIN full polarization data are also shown on Figure 5a.

https://doi.org/10.1017/S1743921307013166 Published online by Cambridge University Press

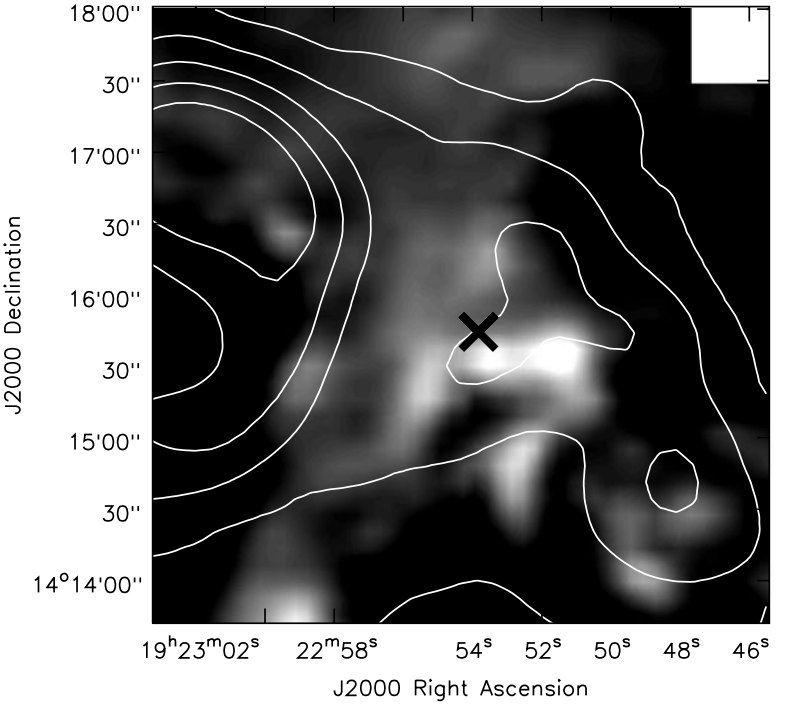

Figure 6. Greyscale of the shocked CO(3–2) integrated intensity with the 90cm continuum contours from Fig. 4 superposed in white. The positions of the OH (1720 MHz) masers are marked by the black × symbol (Brogan et al. in prep.).

From a diverse set of archival and new multi-wavelength data we have determined that (1) there is a 20 and 90cm continuum enhancement at the position of the maser spots with an angular size of $\sim 1.5'$; (2) this enhancement is encircled by a ring of shocked CO(3–2) emission (Figure 6); and (3) there is weak, hard X-ray emission at the same location (Koo *et al.* 2005). These data suggest two possibilities: either the continuum emission, shock, and X-rays are due to W51C (which lies behind W51B) or along this crowded line of sight there is a previously unknown small supernova remnant in front of (or co-distant with) the W51B H II regions. As will be explained in more detail in Brogan *et al.* (in prep.), we favor the second explanation. Comparison of the North-South orientation of the ring of shocked CO(3–2) and 90cm continuum emission in the vicinity of the masers (Fig. 6, note the orientation of the filament in this region is clearer in the channel maps, not shown) and the orientation of the χ^{maser} (Fig. 5) suggest that similar to the case of W44, the linear polarization vectors of the OH (1720 MHz) W51C masers are aligned with the shocked filament, and by association with the direction of the plane-of-sky component of the magnetic field (note this is a bit clearer in the channel maps, not shown).

3. Implications

Maser theories suggest that χ^{maser} will either be parallel or perpendicular to the magnetic field direction in the plane-of-the-sky ($B_\perp$) (see e.g. Elitzur 1998, Watson & Wyld 2001). Furthermore, these theories also show that for the case where $\chi^{maser} \| B_\perp$ the angle to the line-of-sight component of the magnetic field ($B_\|$) is $< 55°$ and that $B_\| > 55°$ for the case where $\chi^{maser} \perp B_\perp$. The fact that some sources fall into the $\chi^{maser} \| B_\perp$

https://doi.org/10.1017/S1743921307013166 Published online by Cambridge University Press

case and some the $\chi^{maser} \perp B_{\perp}$ breaks the uncomfortable coincidence pointed out by Brogan *et al.* (2000) that since all SNR OH (1720 MHz) masers have linear polarization percentages of $\sim 10\%$ they could all have essentially the same $B\|$ which is extremely unlikely. The work of Watson & Wyld (2001) further suggests that the value measured for B_θ is also a function of the degree of maser saturation, though the specific J transition appropriate for OH (1720 MHz) masers has not yet been modeled. The brightness temperatures of these masers $T_b \sim 10^{8-10}$ K, along with the lack of significant variability, are consistent with at least a moderate degree of saturation. For moderate saturation, Watson & Wyld (2001) find that at least for the J = 1–0 and 2–1 transitions the Zeeman equation $V = (Z/2)BdI/d\nu$ (Z = the Zeeman coefficient, and B is the total field strength) with no assumed θ dependence is approximately correct, i.e. $B \approx B_\theta$.

From these data we have also learned that SNR OH (1720 MHz) masers exhibit a core/halo morphology with 50%-80% resolved out by MERLIN and then another 50%-80% by the VLBA. The comparatively large intrinsic scalesizes measured for these masers ($\sim 10^{14-15}$ cm) is in agreement with collisional pump theories (Wardle 1999, Lockett *et al.* 1999). We also find that the small increases observed in the magnetic field strengths with decreasing resolution can be fully explained by spatial/spectral blending effects, and do not appear indicative of tangled B fields.

References

Brogan, C. L., Frail, D. A., Goss, W. M., & Troland, T. H. 2000, *ApJ*, 537, 875
Claussen, M., Frail, D. A., Goss, W. M., & Gaume, R. A. 1997, *ApJ*, 489, 143
Claussen, M. J., Frail, D. A., Goss, W. M., & Desai, K. 1999a, *ApJ*, 522, 349
Claussen, M. J., Goss, W. M., Frail, D. A., & Seta, M. 1999b, *AJ*, 117, 1387
Claussen, M. J., Goss, W. M., Desai, K. M., & Brogan, C. L. 2002, *ApJ*, 580, 909
Dickel, J. R., & Milne, D. K. 1976, Australian Journal of Physics, 29, 435
Elitzur, M. 1976, *ApJ*, 203, 124
Elitzur, M. 1998, *ApJ*, 504, 390
Frail, D. A., Goss, W. M., Reynoso, E. M., Giacani, E. B., Green, A. J., & Otrupcek, R. 1996, *AJ*, 111, 1651
Frail, D. A., Goss, W. M., & Slysh, V. I. 1994, ApJ, 424, L111
Frail, D. A., & Mitchell, G. F. 1998, *ApJ*, 508, 690
Goss, W. M. & Robinson, B. J. 1968, *ApL*, 2, 81
Green, A. J., Frail, D. A., Goss, W. M., & Otrupcek, R. 1997, *AJ*, 114, 2058
Hoffman, I. M., Goss, W. M., Brogan, C. L., Claussen, M. J., & Richards, A. M. S. 2003, *ApJ*, 583, 272
Hoffman, I. M., Goss, W. M., Brogan, C. L., & Claussen, M. J. 2005a, *ApJ*, 620, 257
Hoffman, I. M., Goss, W. M., Brogan, C. L., & Claussen, M. J. 2005b, *ApJ*, 627, 803
Koo, B. -C., Kim, K. -T., & Seward, F. D. 1995, *ApJ*, 447, 211
Koo, B.-C., Lee, J.-J., Seward, F. D., & Moon, D.-S. 2005, *ApJ*, 633, 946
Koralesky, B., Frail, D. A., Goss, W. M., Claussen, M. J., & Green, A. J. 1998, *AJ*, 116, 1323
Lockett, P., Gauthier, E., & Elitzur, M. 1999, *ApJ*, 511, 235
Velázquez, P. F., Dubner, G. M., Goss, W. M., & Green, A. J. 2002, *AJ*, 124, 2145
Wardle, M., 1999, *ApJ*, 525, L101
Watson, W. D., & Wyld, H. W. 2001, *ApJ*, 558, L55
Wolszczan, A., Cordes, J. M., & Dewey, R. J. 1991, *ApJ*, 372, L99
Yusef-Zadeh, F., Goss, W. M., Roberts, D. A., Robinson, B., & Frail, D. A. 1999, *ApJ*, 527, 172
Yusef-Zadeh, F., Roberts, D. A., Goss, W. M., Frail, D. A., & Green, A. J. 1996, *ApJ*, 466, L25
Yusef-Zadeh, F., Wardle, M., & Roberts, D. A. 2003, *ApJ*, 583, 267